Soft Matter

PAPER

View Article Online
View Journal | View Issue

Check for updates

Cite this: *Soft Matter*, 2020, **16**, 7342

Influence of salt concentration on the formation of Pickering emulsions

David J. French,*[a] Jeff Fowler,[b] Phil Taylor[c] and Paul S. Clegg [a]

Received 23rd February 2020,
Accepted 8th July 2020

DOI: 10.1039/d0sm00321b

rsc.li/soft-matter-journal

Here we study emulsification in a model experimental system comprised of water, an oil and colloidal particles. The particles are charge-stabilised colloidal silica; unsurprisingly, by varying the concentration of salt the degree of flocculation of the particles can be modified. The influence of salt on the formation of particle-stabilised oil droplets goes well beyond considerations of the colloidal stability of the particles. Our results demonstrate that the influence of salt on the particle–particle interaction is less important for emulsion formation than the influence of salt on both the particle wettability and the particle–interface interaction.

Open Access Article. Published on 08 July 2020. Downloaded on 7/30/2025 1:54:02 PM.
This article is licensed under a Creative Commons Attribution-NonCommercial 3.0 Unported Licence.

1 Introduction

In previous studies we have developed a model particle-stabilised oil-in-water emulsion in which we can control whether droplets are coated by a monolayer of colloidal particles or whether the particles are shared between two droplets (to form a particle bridge).[1,2] One route to avoiding bridge formation is to add salt to the system. Here we deploy our well-controlled system to investigate the process of the formation of Pickering emulsions in the presence of salt but in the absence of colloidal bridges.

Initially the presence of salt has a variety of effects prior to and during emulsification. The Debye length in the aqueous phase is reduced, meaning electrostatic interactions are more strongly screened, and both the viscosity and refractive index of the water are increased.[3–5] Reducing the Debye length may lead to the particles aggregating through van der Waals attractions. The addition of salt to the aqueous phase also increases the rate of coalescence between oil droplets which are not fully coated with particles, as the oil droplets carry a slight charge.[6] This is important, as a slower coalescence rate allows the particles more time to adsorb to an oil–water interface, yielding smaller and more stable droplets. Finally, if the particles carry the opposite sign of charge to the oil–water interfaces, then adsorption will be hindered by the presence of salt.

Once the emulsion has formed, salt has an influence on the final position of trapped particles as described by, θ_w, the three-phase contact angle.[7] The change in free energy, ΔG, occurring when a particle moves from its preferred phase to the oil–water interface is given by:

$$\Delta G = -\pi r_p^2 \sigma_{ow}(1 - |\cos\theta_w|)^2, \quad (1)$$

where r_p is the particle radius and σ_{ow} is the oil–water interfacial tension.[8] This change is typically large enough to lead to irreversible trapping, although bridging can modify this situation.[2] It has been predicted theoretically that θ_w for silica particles at an oil–water interface will decrease (*i.e.* the particles will become more hydrophilic) when the sodium chloride concentration of the aqueous phase is increased.[9,10] Since the electrical double layer forms spontaneously, its formation must reduce the system's free energy. Therefore, when the salt concentration is increased, the system can lower its free energy by increasing the solid–water interfacial area, as this increases the contact area of the double layer. Fokkink and Ralston also show that θ_w is at a maximum (*i.e.* the particles are most hydrophobic) at the isoelectric point of the solid surface, and that θ_w will decrease as the magnitude of the surface potential is increased. We have previously used the sessile drop method to show that our particles do indeed become more hydrophilic as the sodium chloride concentration of the aqueous phase is increased.[1]

Gautier *et al.* studied the effects of changing both pH and the sodium chloride concentration of the aqueous phase in emulsions stabilised by silica and latex particles.[11] They observed several interesting phenomena, including bidisperse droplet populations at intermediate salt concentrations and droplet surface coverages which were substantially below that of hexagonal close packing at high pH and low salt concentrations. Below we consider the role of salt on emulsion formation in isolation, we study a broader range of salt concentrations and we show the contrasting behaviour of sodium chloride and sodium iodide. We also employ fluorescently labelled silica

[a] *School of Physics & Astronomy, The University of Edinburgh, Peter Guthrie Tait Road, Edinburgh EH9 3FD, UK. E-mail: David.French@ed.ac.uk*
[b] *Syngenta Inc., 410 Swing Rd, P.O. Box 183000, Greensboro, North Carolina, 27419-8300, USA*
[c] *Formulation Technology Group, Syngenta Crop Sciences, Jealotts Hill International Research Centre, UK*

This journal is © The Royal Society of Chemistry 2020

Open Access Article. Published on 08 July 2020. Downloaded on 7/30/2025 1:54:02 PM.
This article is licensed under a Creative Commons Attribution-NonCommercial 3.0 Unported Licence.

particles and confocal microscopy which allows us to extend our work to higher particle volume fractions.

2 Materials and methods

2.1 Materials

Distilled water, deionised using a Millipore Milli-Q system to a resistivity $\geq$18 MΩ cm, was used throughout. Dodecane (Sigma-Aldrich, $\geq$99%) and isopropyl myristate (Sigma-Aldrich, $\geq$98%) formed the oil phase. The dodecane was filtered through an alumina column twice to remove polar impurities. Isopropyl myristate was used as received, as were sodium chloride (VWR, 99.9%) and sodium iodide (Sigma-Aldrich, 99.5%).

2.1.1 Silica particles. The synthesis of Stöber silica particles was carried out by Dr Andrew Schofield following ref. 12. Incorporation of a fluorescent dye is *via* the coupling agent 3-(aminopropyl)triethoxysilane (APS) which is added in excess. The APS contributes amino groups, which are positively charged below pH $\approx$ 9, to the particle surface. The native silanol groups are negatively charged above pH $\approx$ 2. The actual charge on the particle depends on the ratio of silanol to amino groups, and varies with pH.[13] Static light scattering (Section 2.2.2) showed that the particle radius r_p = 430 nm. The particles' zeta potential, ζ, was measured (Section 2.2.4) immediately following dispersion in deionised water and again following immersion in water for 24 h. Immediately following dispersion, $\zeta \approx 40$ mV, and 24 h later $\zeta \approx -5$ mV. To avoid this time dependence, all emulsification was carried out within 10 min of particle dispersion.

2.2 Particle phase behaviour: sample preparation

2.2.1 Dispersion preparation. The silica particles were washed ten times with distilled water to remove the ammonia, and then dried for one hour in a vacuum oven pre-heated to 170 °C, rendering the particles hydrophobic enough to sequester to the oil–water interface.[14]

Dried silica particles and salt were dispersed in 2.33 mL of water using ultrasound (Sonics Vibracell VCX500). A typical protocol was 1 s of sonication then 5 s rest, repeated for a total time of 6 min, at an amplitude of 20% of instrument maximum. A typical sample, with ϕ_p = 1.7% and [NaCl] = 100 mM contained 0.09 g of silica and 0.014 g of NaCl.

2.2.2 Particle and droplet sizing. A Beckman Coulter LS 13 320 Particle Size Analyzer was used to characterise the emulsion droplets and aggregates as well as the apparent particle size in silica dispersions with time. A fresh dispersion of particles with volume fraction of 0.3% was prepared without any salt for each experiment. The sizing module contains $\approx$20 mL of aqueous phase with the desired salt concentration, to which $\approx$1 mL of particle dispersion was added; the change in salt concentration was considered low enough to be neglected. This protocol minimises the amount of aggregation which occurs prior to initial measurement, although the loading of the sample took $\approx$1–2 min. To prevent the particles from coating the inner walls of the module, the stirrer bar was rotated at a constant rate (50% of instrument maximum) for all the experiments. The initial obscuration was 10%.

An ALV/CGS-3 goniometer and an ALV-5004 Multiple Tau Correlator were used to perform static light scattering measurements in order to measure the size of the Stöber silica particles. Calculation of r_p was done by fitting the minima in the form factor to:

$$q_p r_p = \tan(q_p r_p), \quad (2)$$

where q_p is given by:

$$q_p = \frac{4\pi n}{\lambda}\sin\left(\frac{\alpha}{2}\right), \quad (3)$$

and n is the refractive index of the solvent, λ is the wavelength of light being scattered and α is the scattering angle.[15]

2.2.3 Sedimentation behaviour. The flocculation behaviour of the particles can also be seen from sedimentation profiles. A series of particle dispersions varying in sodium chloride concentration was prepared and photographs were taken using Qimaging's QCapture Suite software and a Qimaging QICAM Fast 1394 monochromatic camera with a telescopic lens attachment. When a sharp sedimentation front is visible, Stokes' law can be used to estimate the particles' radius from their sedimentation velocity, to indicate the degree of aggregation in a sample. The terminal velocity, v_t, of a spherical particle of density, ρ_p, sedimenting in a fluid of viscosity, η, and density, ρ_f, is given by:

$$v_t = \frac{2{r_p}^2\left(\rho_p - \rho_f\right)g}{9\quad\eta}, \quad (4)$$

where g is the acceleration due to gravity.[16]

Particle dispersions with various aqueous phase concentrations of sodium chloride and sodium iodide were observed, with ϕ_p = 0.35%. The dried particles and salt were dispersed in 15 mL of deionised water using the ultrasonic probe.

2.2.4 Zeta potential. The zeta potential of particle dispersions were measured using a Malvern Nano-Z ZEN2600 Zetasizer. Particle dispersions for zeta potential measurements were prepared by adding $\approx$0.005 g of particles to $\approx$3 mL of deionised water containing 1 mM of sodium nitrate (Sigma-Aldrich, $\geq$99.0%), and dispersing with the ultrasonic probe. The addition of the salt ensures that the Debye length is much smaller than r_p.

2.3 Emulsion characterization

2.3.1 Sample preparation. Eight oil-in-water emulsion samples were prepared, each with ϕ_p = 1.7% and ϕ_o = 20%. The oil phase (0.67 mL) was a mixture of a non-polar and a polar oil; specifically, the volume fraction of isopropyl myristate relative to dodecane was set at Φ_{IM} = 10% to control particle wettability.[17] We assume that the density of the oil phase is 760 kg m^{-3}. Dispersions of silica were typically prepared as above. The sodium chloride concentrations were 0 mM, 10 mM, 30 mM, 100 mM, 300 mM, 750 mM, 1500 mM and 4000 mM – covering non-flocculating, weakly flocculating and strongly flocculating dispersions. Emulsification using a vortex mixer (Fisons Whirlimixer) was carried out within 10 min of the particles being added to the water. Unless otherwise stated, the samples were vortex mixed until the resolved water was clear, or until further mixing did not decrease the opacity of the resolved water.

The samples were photographed regularly as the droplets creamed and any remaining particles sedimented. The droplet

Open Access Article. Published on 08 July 2020. Downloaded on 7/30/2025 1:54:02 PM.
This article is licensed under a Creative Commons Attribution-NonCommercial 3.0 Unported Licence.

size distribution (measured using light scattering) was used to characterise the emulsion formation process; an increase in the droplet size indicates that more coalescence occurred during emulsification. If, for a given sample preparation route, the droplet size is small, then the emulsification process has been more efficient than if the same preparation route led to a large droplet size. To provide more insight, slides were prepared, with a drop of emulsion from each sample being diluted in some of the sample's continuous (aqueous) phase for optical and confocal microscopy.

2.3.2 Imaging. A Qimaging QICAM Fast 1394 monochromatic camera, attached to an Olympus BX50 optical microscope, was used to obtain bright-field images of emulsions. A Zeiss LSM 700 confocal microscope was also used with a 10 mW, 488 nm solid-state laser to excite the FITC dye. Generally, a 10× objective was used, which is just powerful enough to resolve individual particles, but gives a large field-of-view. High resolution microscopy was performed using a 40× or 63× oil immersion objective.

2.3.3 Droplet sizing. The particle size analyzer was filled using the continuous phase of the sample being studied, and drops of sample were added until the obscuration was within the suggested range. Three measurements (1 min each) were generally made for each sample, and averaged. Unless otherwise stated, the volume-weighted size distribution has been used. The stirrer bar was operated at 50% of instrument maximum speed.

The droplet size has been used to characterise emulsion stability; an increase in the droplet size indicates that more coalescence occurred during emulsification, either because the particle trapping energy is lower or because the particles are not able to adsorb to the interface during emulsification. If, for a given sample preparation route, the droplet size is small, then the emulsification process has been more efficient than if the same preparation route led to a large droplet size. Since optimising the emulsion system so that the emulsification process requires as little energy as possible is desirable, small droplet size can be used to indicate success.

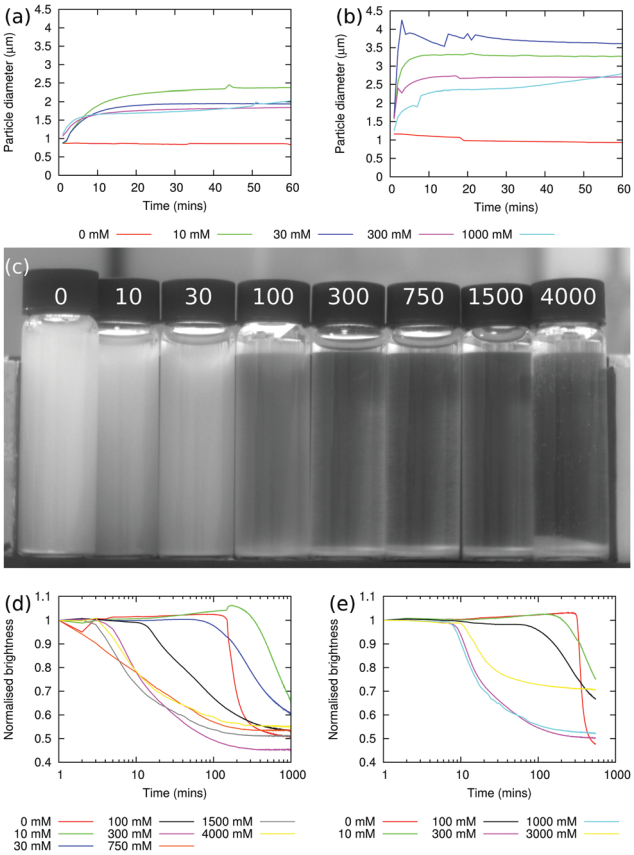

Fig. 1 NaCl & NaI (a) and (b) Aggregation behaviour of dispersions of silica particles under shear at different sodium chloride (a) and sodium iodide (b) concentrations. (c) Photograph of Stöber silica dispersions after 120 min of sedimentation. The sodium chloride concentrations, in mM, are shown on each vial and ϕ_p = 0.35% in all samples. (d) and (e) Graphs showing the normalised brightness (a lower normalised brightness means that more particles have sedimented) as a function of time for the dispersions containing sodium chloride (d) and sodium iodide (e).

3 Results

3.1 Characterization of particle flocculation

The sizes of particle aggregates are shown in Fig. 1(a) for sodium chloride and Fig. 1(b) for sodium iodide. When there is no added salt, the apparent particle size does not increase over the course of the experiment, which lasted 1 h, showing that the particles are indeed non-aggregating under these conditions (in fact, the particle size decreases slightly over the course of the experiment, as aggregates which were not initially fully dispersed are broken up). At non-zero salt concentrations, the apparent particle size increases relatively quickly over the first 5–10 min of the experiment, and then plateaus. The plateau value typically decreases as the salt concentration is increased, and this may be caused by the increased viscosity at higher salt concentrations leading to a greater shear stress in the stirred sample. At the highest sodium chloride concentration used here, 1000 mM, the apparent particle size starts to increase again after ≈30 min, suggesting that the particle–particle interactions at this salt concentration are strong enough to overcome the shear rate.

Fig. 1(b) shows that the aggregation behaviour in the sodium iodide samples is qualitatively similar to the sodium chloride case. However, the rate of aggregation at short times is greater and the size of the aggregates in the plateau region is larger. Given the small difference between the viscosities of sodium chloride and sodium iodide solutions at concentrations below ≈500 mM,[3,5] it seems more likely that the differences are due to ion specific effects. Since iodide ions are more chaotropic than chloride ions,[18,19] the concentration of anions which adsorb at particle surface will be lower for iodide than for chloride, and this in turn means that the particle surface charge is likely to be higher for sodium chloride; by contrast, the degree of screening is likely to be higher for sodium iodide. The balance of these two effects will determine how strongly the particles aggregate.

3.1.1 Sedimentation behaviour. With no added salt, the particles sedimented slowly initially, until ≈5 h, when they aggregate and sediment rapidly, with full sedimentation (≈6 cm) taking about another hour. This behaviour is due to

This journal is © The Royal Society of Chemistry 2020

Open Access Article. Published on 08 July 2020. Downloaded on 7/30/2025 1:54:02 PM.
This article is licensed under a Creative Commons Attribution-NonCommercial 3.0 Unported Licence.

a change in the zeta potential of the particles which is related to water adsorption.[20] In the initial phase, the particles sediment $\approx$0.53 cm in the first 275 min; Stokes' equation gives r_p = 440 nm, in good agreement with light scattering (r_p = 430 nm).

When particle aggregation, due to the presence of salt, is superimposed on sedimentation, the interface between the sediment and the supernatant is no longer sharp. The average brightness, $b(t)$, of each sample has been measured using the Plot Profile feature in ImageJ to select rectangular sections covering as much of each vial as possible. This is then repeated for multiple photographs taken at different times, with t being the time elapsed since the beginning of the experiment.[21] In order to account for changing light conditions $b(t)$ is also normalised by dividing by the average brightness of two sections of the photograph, one in the background and one in the foreground. A typical photograph from this experiment is shown in Fig. 1(c) (this photograph has been cropped such that the background and foreground sections used for normalisation aren't visible[20]). By plotting $b(t)/b(t = 0)$ as a function of t, the sedimentation behaviour can be seen. Fig. 1(d) shows such a plot for dispersions containing sodium chloride. The sudden onset of sedimentation in the 0 mM sample can clearly be seen.

At higher salt concentrations, 10–30 mM, the dispersions are observed to sediment at approximately the same rate as in the sample without salt. However, in the presence of salt, the particles do not all aggregate rapidly after $\approx$5 h, but gradually aggregate and sediment over the course of $\approx$20 h. At still higher concentrations of sodium chloride, 300–4000 mM, aggregation occurs immediately and the particles sediment rapidly, with sedimentation taking less than an hour.

Fig. 1(e) shows the results of a similar experiment using sodium iodide. No qualitative differences between dispersions containing sodium chloride and sodium iodide were observable.

3.2 Characterization of droplet size

3.2.1 Sodium chloride. A photograph of the samples prepared using sodium chloride, Fig. 2(a), shows that the emulsion stability changes dramatically with sodium chloride concentration. No further changes to the samples are observed if they are left for several weeks.

The size distributions of the emulsions in Fig. 2(a) are shown in Fig. 2(b), and Fig. 3 shows the average droplet size from these samples. The droplet size appears smallest when [NaCl] = 10 mM. However, this is because the droplets in the 0 mM sample are aggregating due to particle bridging.[1] Hence as [NaCl] is increased from 0 mM to 1500 mM, the emulsion droplets get continuously larger, *i.e.*, the particles are becoming increasingly ineffectual. This might be because the salt screens the particle-interface attraction during mixing, so that particles are less likely to adsorb to the interface and/or because the particle trapping energy has decreased.

Bright-field microscopy confirms the light-scattering data, see Fig. 2(b)–(h) and Fig. 3. The situation is slightly more complicated than Fig. 3 might initially suggest. At the lowest salt concentrations, $\lesssim$10 mM, the emulsion is relatively monodisperse. However, at a salt concentration of $\approx$30 mM, the

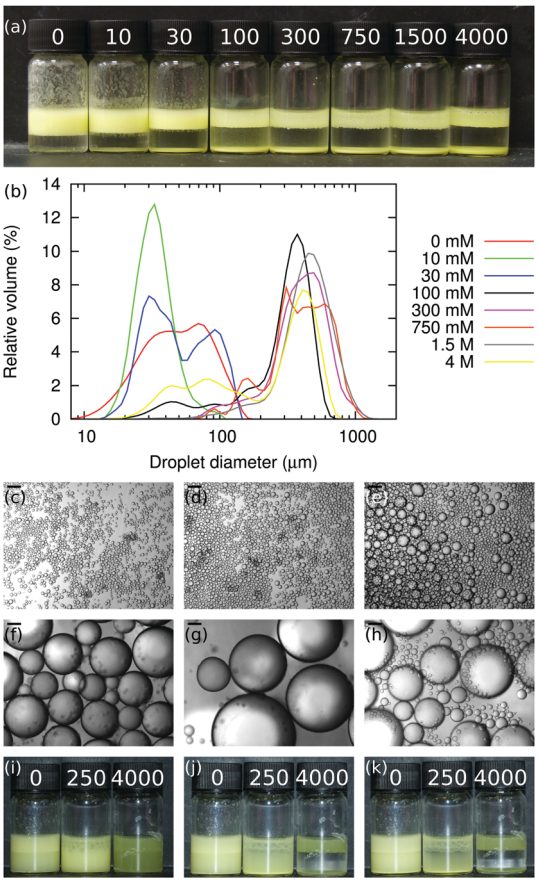

Fig. 2 NaCl (a) Photograph showing emulsions stabilised by Stöber silica (yellow due to FITC dye) at various sodium chloride concentrations (on vial, mM). The amount of free silica at the base of the vial increases with salt concentration. (b) Size distributions of emulsions at various sodium chloride concentrations. In all samples, ϕ_p = 1.7%, ϕ_o = 20% and Φ_{IM} = 10%. (c)–(h) Micrographs of emulsions at sodium chloride concentrations of 0 mM, 10 mM, 30 mM, 100 mM, 300 mM and 4000 mM. The scale bars are 100 μm. (i)–(k) Photographs of emulsions at salt concentrations shown on each vial, mM. In all three samples ϕ_p = 1.1%, ϕ_o = 20% and Φ_{IM} = 0%. The times since emulsification are 0, 40 and 80 min.

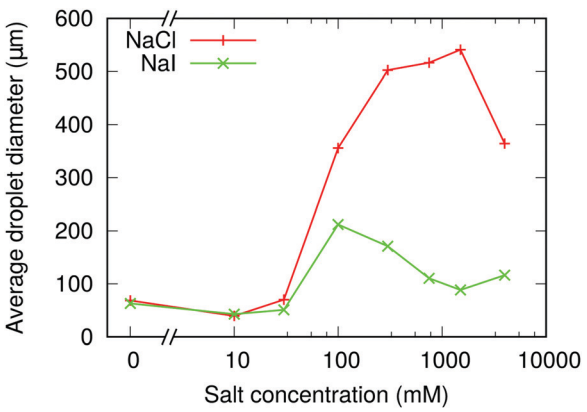

Fig. 3 NaCl & NaI: volume-weighted mean droplet size of emulsions at different sodium chloride and sodium iodide concentrations. In all samples, ϕ_p = 1.7%, ϕ_o = 20% and Φ_{IM} = 10%.

Open Access Article. Published on 08 July 2020. Downloaded on 7/30/2025 1:54:02 PM.
This article is licensed under a Creative Commons Attribution-NonCommercial 3.0 Unported Licence.

emulsion becomes bidisperse, with two populations of droplets with mean diameters of ≈30 μm and 100 μm. At still-higher salt concentrations the size distribution becomes monodisperse again, with droplet diameters centered on ≈500 μm in the range 100–1500 mM, before becoming bidisperse again at the highest salt concentration studied here (4000 mM), where the droplet populations are centered around ≈80 μm and ≈500 μm.

Along with the changes in droplet size, an increase in free silica is observed when [NaCl] increases, as seen in Fig. 2(a) and (b). We attribute this to sodium chloride altering the contact angle, decreasing it initially. This means that particles are less likely to adsorb to the oil–water interface during emulsification (due to salt screening the particle-interface attraction) and that particles which do adsorb will be less strongly trapped at the oil–water interface (due to salt lowering θ_w). The weaker particle adsorption also means that as limited coalescence progresses, particles may be ejected from the interface either during the coalescence events themselves, or soon afterwards as jammed particles at the interface of a non-spherical droplet relax.

3.2.2 Surface coverage. Optical and confocal microscopy reveal differences in how the particles arrange themselves at a droplet's surface. At very low [NaCl] (≤10 mM), the droplets are generally fully covered and the particles form a monolayer at the oil–water interface, see Fig. 4(a). When [NaCl] is increased to 30 mM, droplets with surface coverage well below close-packing are observed (Fig. 4(b)). These are generally the larger droplets in the sample, suggesting that there is a link between the appearance of a bidisperse size distribution at this salt concentration, and the lower surface coverage observed. Evidently the particles on the droplet in Fig. 4(b) are aggregating, which is consistent with the dispersion behaviour. At [NaCl] greater than ≈100 mM, the particle layer at the oil–water interface is no longer a monolayer, but instead extends significantly into the aqueous phase, as shown in Fig. 4(c) and (d). Clearly, the efficiency of the particle stabilization is reduced here.

We also note that at [NaCl] = 30 mM, Fig. 2(a), not all of the particles adsorb to an interface, and a significant fraction of the particles sediment in the aqueous phase. Nonetheless, some droplets are left with large bare patches on their surfaces and are yet stable against further coalescence. Given the salt concentration in this sample, it seems unlikely that charged interfaces could be responsible for stabilizing the droplets. Alternatively, the particle attractions might be strong enough that particles on opposing droplets migrate on their respective interfaces so that they are closer together as droplets come into contact.

Overall, as [NaCl] is increased, the droplets change from being fully coated by particles to being partially coated by aggregated particles (see also ref. 22), and then to being fully coated by particles, but with particle layers which extend into the continuous phase, see cartoon in Fig. 4(e). The change from being fully coated to being partially coated appears to coincide with the change from a non-flocculating dispersion to a weakly flocculating dispersion, where the emulsification process is still capable of breaking up the particle aggregates but where screening of the particles' charge leads to lowered particle adsorption rates and particle trapping energies. The appearance of bidisperse emulsions may be related to this; small droplets could be stabilised by dispersed particles whilst the larger droplets are stabilised by clusters of particles. The transition to a system where the particles in the continuous phase form a network linking droplets together may then occur at the point where the emulsification process is no longer capable of fully disrupting particle aggregates. The increase in particle–particle attraction on droplet interfaces as [NaCl] is increased may be responsible for an enhanced coalescence rate at higher salt concentrations leading back to fully coated droplets.

As well as the thickening of the particle layer at the interface, the amount of sedimented silica increases with [NaCl], see Fig. 2(a). Together, these contribute to the increased droplet size. The increase in the packing fraction of the emulsions as the salt concentration increases from 0 mM to 30 mM is evidence of particle bridging in the low salt concentration samples.[1] The resulting dependence of droplet size on [NaCl] is non-monotonic, Fig. 5, independent of the availability of particles.

3.2.3 Sodium iodide. Fig. 6(a) shows a photograph of samples at a variety of sodium iodide concentrations with size distributions in Fig. 6(b). A graph showing the volume-weighted mean droplet diameters for both salts is shown in Fig. 3. The effect of including sodium iodide is broadly similar to that of including sodium chloride, in that the average droplet size is lowest at small salt concentrations, passes through a peak at intermediate salt concentrations and decreases again at higher salt concentrations, see micrographs in Fig. 6(c)–(h). The key differences between salts are, firstly, the mean droplet size in

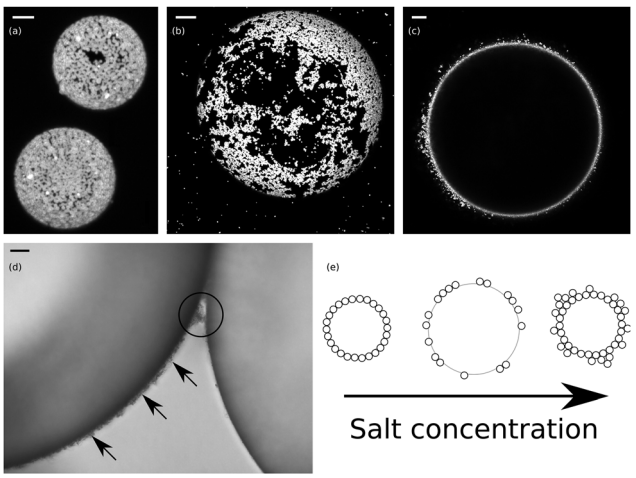

Fig. 4 NaCl (a) Confocal micrograph z-projection of 14 images, with a z-spacing of 0.44 μm (ImageJ[21]) showing the particle layers at two droplet interfaces. [NaCl] = 10 mM; the scale bar is 5 μm. (b) Confocal micrograph z-projection of 42 images, with a z-spacing of 0.44 μm showing the packing of particles at the interface. [NaCl] = 30 mM; the scale bar is 20 μm. (c) Confocal micrograph showing the thickened particle layer at the interface in the 100 mM sample. The scale bar is 20 μm. (d) Micrograph showing the thickening of the interfacial particle layer. The arrows indicate the thickened particle layer, which protrudes several micrometres into the continuous phase and the circled area shows that the layer can be shared by droplets. [NaCl] = 300 mM; the scale bar is 10 μm. (e) Cartoon summarizing the behaviour of droplets as the salt concentration is increased, see text.

This journal is © The Royal Society of Chemistry 2020

Open Access Article. Published on 08 July 2020. Downloaded on 7/30/2025 1:54:02 PM.
This article is licensed under a Creative Commons Attribution-NonCommercial 3.0 Unported Licence.

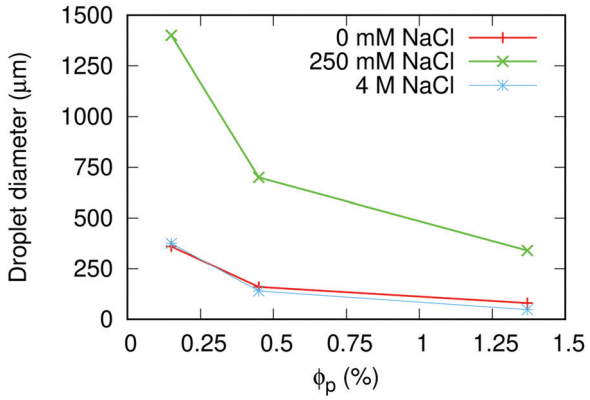

Fig. 5 NaCl volume-weighted median droplet size at different [NaCl] and particle volume fractions, ϕ_p. Measurements were made using light scattering, except for the lower two ϕ_p at [NaCl] = 250 mM, which were estimated from photographs. All samples had Φ_{IM} = 0% and were emulsified using a vortex mixer for 30 s each.

the emulsions containing sodium iodide is smaller at all salt concentrations, and considerably smaller at high salt concentrations. Secondly, bidisperse distributions are obvious at all sodium iodide concentrations in the range 30–4000 mM whereas these are only observed at sodium chloride concentrations of 30 mM and 4000 mM, but not in between.

The dramatic difference in the size of the droplets in emulsions which contain the same molarity of sodium chloride and sodium iodide is initially surprising. As was shown above, the particle dispersions containing sodium iodide aggregate more strongly than dispersions containing an equal molarity of sodium chloride, especially when sheared, an effect we attribute to iodide ions being more chaotropic than chloride ions. Particle adsorption rates have been shown to change with particle size, although the relevance of these results to high Reynolds number systems remains to be demonstrated.[7,23] Since the coalescence rate also increases as salt is added, a small difference in the particle adsorption rate may make a relatively large difference to the eventual droplet size.

3.2.4 Surface coverage. As with the samples containing sodium chloride, changes in the surface coverage of emulsion droplets were observed as the sodium iodide concentration was increased. When no salt was added the droplets were generally fully covered, as before. At small [NaI] ($\lesssim$30 mM), the surface coverage was observed to be a monolayer with very few gaps, Fig. 7(a). When [NaI] is increased to 100–750 mM, the particle layer at the interface was again observed to thicken slightly in some places,

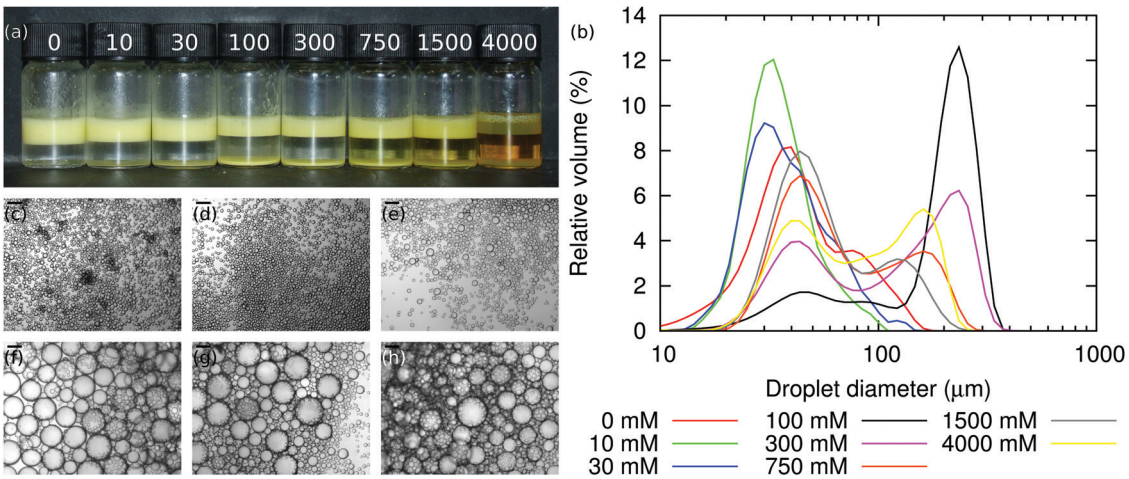

Fig. 6 NaI (a) Photograph showing emulsions stabilised by Stöber silica at [NaI] given in mM on each vial. The amount of free silica can clearly be seen to increase with salt concentration. (b) Size distributions of emulsions stabilised by Stöber silica at various [NaI]. (c)–(h) Micrographs of emulsions stabilised by Stöber silica at [NaI] of 0 mM, 10 mM and 30 mM, 100 mM, 300 mM and 1500 mM. The scale bars are 100 μm.

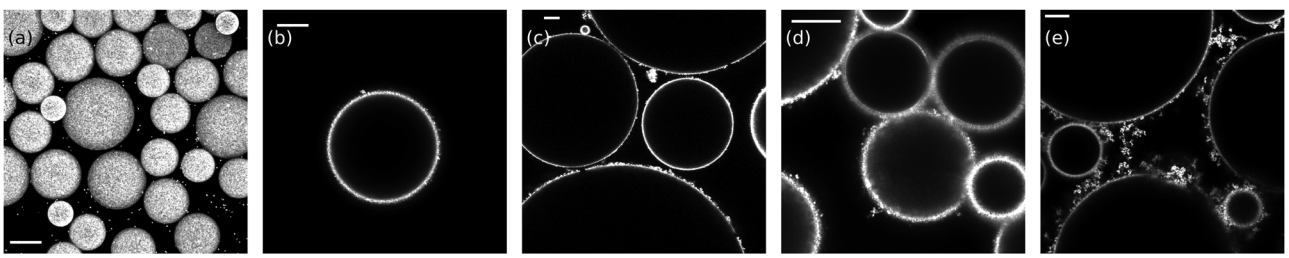

Fig. 7 NaI (a) A z-projection of 17 confocal micrographs, with a z-spacing of 0.44 μm, constructed using ImageJ with [NaI] = 30 mM.[21] (b)–(e) Confocal micrographs showing surface coverage of emulsion droplets stabilised by Stöber silica, with [NaI] of 100 mM, 300 mM, 750 mM and 1500 mM, respectively. The thickening of the particle layer at the droplets' interface as the salt concentration is increased can clearly be seen. The scale bars are 20 μm.

Open Access Article. Published on 08 July 2020. Downloaded on 7/30/2025 1:54:02 PM.
This article is licensed under a Creative Commons Attribution-NonCommercial 3.0 Unported Licence.

Fig. 7(b)–(d), so that the particle aggregates protruded slightly into the continuous phase. As with the sodium chloride case, when [NaI] was increased to $\geq$1500 mM, the particle aggregates protruded extensively into the continuous phase, such that the emulsion droplets were almost all connected to each other by a network of aggregated particles, as can be seen in Fig. 7(e). Such network formation in the continuous phase of a particle-stabilised emulsion has been noted previously.[24,25]

Unlike the sodium chloride case, partially coated droplets are not observed in any of the sodium iodide samples. This is surprising because the particles which remain in the continuous phase form an open and branched network. This may be because θ_w is high enough that the adsorbed particles repel due to electrostatic forces mediated through the oil phase.[26,27] Since not all of the particles adsorb to an oil–water interface, but the droplets become fully covered by particles, the increase in droplet size observed at intermediate [NaI] can be attributed to the increased coalescence rate between droplets, which is caused by the increased screening of electrostatic charge present at the droplet interfaces. Alternatively, as discussed below, the internal structure of particle flocculations formed in NaI may be rather different than those formed in weakly flocculating, intermediate [NaCl], and this could also explain the observed differences in the extents to which droplets are covered.

4 Discussion

4.1 Particle flocculation

The observations presented are roughly in-line with expectations, but for these to illuminate emulsion formation they must be put alongside two other points. (1) The degree of aggregation in a particle dispersion will depend not only on the particle interactions, and hence the influence of salt, but also on the shear stress in the fluid. Consequently, an important factor will be whether the applied shear is capable of breaking up the particle aggregates. In this context, note the upward trend in the aggregate size at experimental times greater than 30 min and when the salt concentration is 1 M, as shown in Fig. 1(a) and (b). In contrast, at salt concentrations $\leq$300 mM the aggregate size is observed to plateau at a salt concentration-dependent value. Therefore, it is argued that at salt concentrations $\leq$300 mM the particle dispersions can be described as weakly flocculating. The aggregation state following shear emulsification and adsorption to an interface may only indirectly reflect the aggregation state observed during low shear sedimentation, but the latter observations still are informative about interparticle forces. (2) The particles initially have a positive zeta potential, but this decreases and eventually becomes negative due to water adsorption at their surfaces.[14,28] It is very likely that this effect is too slow to be important here.

4.2 Droplet size

Oil-in-water Pickering emulsions stabilised by fluorescent Stöber silica have been produced. The most stable emulsions are formed when the aqueous phase contains no salt and the least stable emulsions are formed at [NaCl] $\approx$ 1000 mM; above this concentration the emulsion stability increases. A summary of this behaviour can be seen in Fig. 2(i)–(k), which show emulsions similar to those in Fig. 2(a), but with ϕ_p = 1.1% and Φ_{IM} = 0%. Samples containing sodium iodide are observed to be more stable than those containing an equal concentration of sodium chloride, despite sodium iodide causing the particle dispersions to flocculate more strongly. This is attributed to the iodide ions being more chaotropic than chloride ions, which causes the particles to be more hydrophobic and hence more likely to be trapped at a droplet interface. An alternative explanation may lie in the expected differences in internal structure between weakly- and strongly-bonded flocculations, as reported by Stradner *et al.*,[29] that reasonably might be expected to influence how strongly they adsorb to interfaces, and their propensity to be removed by shear during emulsification. The relevance of these ideas to colloids at interfaces is not at all clear.

It is valuable to focus on the measured droplet size, Fig. 5, as a function of ϕ_p for emulsions generated from non-flocculating, weakly flocculating and strongly flocculating particle dispersions. It can be seen that, for all particle volume fractions, the droplet size is much greater for emulsions created using weakly flocculating particle dispersions than for corresponding emulsions created from non-flocculating and strongly flocculating dispersions. *i.e.* when [NaCl] = 250 mM only a small proportion of the particles have become trapped at the interface. The three [NaCl] shown (0 mM, 250 mM and 4000 mM) correspond to non-flocculating, weakly flocculating and strongly flocculating particle dispersions, as evidenced by the rates at which the free silica sediments (Fig. 2(i)–(k)). Hence, this system behaves in the opposite manner from that described by, for example, Binks and Lumsdon.[30] This discrepancy is likely caused by the differing surface chemistry of the silica particles used here, which have non-native amino groups and fluorescent dye at their surface. Since the fluorescent silica particles are positively charged, there is an attractive interaction between the particles and the oil–water interface. Therefore the addition of salt screens an attractive interaction, making particle adsorption less likely.

5 Conclusions

When Stöber silica is used as the emulsion stabiliser, aqueous phases containing sodium iodide are observed to lead to more stable (having a lower primary droplet size) emulsions than aqueous phases containing sodium chloride. The adsorption of ions at the particle interface is thought to play a rôle in this. For both salts, weakly flocculating particles have been shown to lower the emulsion's stability significantly. This demonstrates that the particle–particle interactions are less important than the particle–interface interactions and, whilst aggregating particles may be an indication that the particles will be attracted to the interface, there is a wealth of other aspects at play here which must be considered.

Conflicts of interest

There are no conflicts to declare.

This journal is © The Royal Society of Chemistry 2020

Open Access Article. Published on 08 July 2020. Downloaded on 7/30/2025 1:54:02 PM.
This article is licensed under a Creative Commons Attribution-NonCommercial 3.0 Unported Licence.

Acknowledgements

We thank A. B. Schofield for synthesising the particles, the EPSRC and Syngenta for a CASE award to D. J. F., and the EPSRC for grant EP/J007404/1.

References

1 D. J. French, P. Taylor, J. Fowler and P. S. Clegg, *J. Colloid Interface Sci.*, 2015, **441**, 30–38.
2 D. J. French, A. T. Brown, A. B. Schofield, J. Fowler, P. Taylor and P. S. Clegg, *Sci. Rep.*, 2016, **6**, 31404.
3 *CRC Handbook of Chemistry and Physics*, ed. D. R. Lide, CRC Press, Boca Raton, 82nd edn, 2001.
4 K. Bai and J. Katz, *Exp. Fluids*, 2014, **55**, 1704.
5 I. M. Abdulagatov, A. B. Zeinalova and N. D. Azizov, *J. Chem. Eng. Data*, 2006, **51**, 1645–1659.
6 K. G. Marinova, R. G. Alargova, N. D. Denkov, O. D. Velev, D. N. Petsev, I. B. Ivanov and R. P. Borwankar, *Langmuir*, 1996, **12**, 2045–2051.
7 *Colloidal Particles at Liquid Interfaces*, ed. B. P. Binks and T. S. Horozov, Cambridge University Press, Cambridge, 2006.
8 J. H. Clint and S. E. Taylor, *Colloids Surf.*, 1992, **65**, 61–67.
9 L. G. J. Fokkink and J. Ralston, *Colloids Surf.*, 1989, **36**, 69–76.
10 R. J. Hunter, *Foundations of Colloid Science*, Clarendon Press, Oxford, 1991, vol. 1.
11 F. Gautier, M. Destribats, R. Perrier-Cornet, J.-F. Dechézelles, J. Giermanska, V. H. S. Ravaine, F. Leal-Calderon and V. Schmitt, *Phys. Chem. Chem. Phys.*, 2007, **9**, 6455–6462.
12 A. Imhof, M. Megens, J. J. Engelberts, D. T. N. de Lang, R. Sprik and W. L. Vos, *J. Phys. Chem. B*, 1999, **103**, 1408–1415.
13 K. A. White, A. B. Schofield, B. P. Binks and P. S. Clegg, *J. Phys.: Condens. Matter*, 2008, **20**, 494223.
14 K. A. White, A. B. Schofield, P. Wormald, J. W. Tavacoli, B. P. Binks and P. S. Clegg, *J. Colloid Interface Sci.*, 2011, **359**, 126–135.
15 P. Pusey and W. van Megen, *J. Chem. Phys.*, 1984, **80**, 3513–3520.
16 H. Lamb, *Hydrodynamics*, Dover Publications, London, 1932.
17 W. J. Frith, R. Pichot, M. Kirkland and B. Wolf, *Ind. Eng. Chem. Res.*, 2008, **47**, 6434–6444.
18 K. D. Collins, *Proc. Natl. Acad. Sci. U. S. A.*, 1995, **92**, 5553–5557.
19 K. I. Assaf and W. M. Nau, *Angew. Chem., Int. Ed.*, 2018, **57**, 13968–13981.
20 D. J. French, PhD thesis, University of Edinburgh, 2015.
21 C. A. Schneider, W. S. Rasband and K. W. Eliceiri, *Nat. Methods*, 2012, **9**, 671–675.
22 M. Derakhshandeh, B. K. Pilapil, B. Workman, M. Trifkovic and S. L. Bryant, *Soft Matter*, 2018, **14**, 4268–4277.
23 D. Reay and G. A. Ratcliff, *Can. J. Chem. Eng.*, 1973, **51**, 178–185.
24 N. Yan and J. H. Masliyah, *Ind. Eng. Chem. Res.*, 1997, **36**, 1122–1129.
25 R. Aveyard, B. P. Binks and J. H. Clint, *Adv. Colloid Interface Sci.*, 2003, **100-102**, 503–546.
26 T. S. Horozov, R. Aveyard, B. P. Binks and J. H. Clint, *Langmuir*, 2005, **21**, 7405–7412.
27 A. D. Law, M. Auriol, D. Smith, T. S. Horozov and D. M. A. Buzza, *Phys. Rev. Lett.*, 2013, **110**, 138301.
28 L. T. Zhuravlev, *Colloids Surf., A*, 2000, **173**, 1–38.
29 A. Stradner, H. Sedgwick, F. Cardinaux, W. C. K. Poon, S. U. Egelhaaf and P. Schurtenberger, *Nature*, 2004, **432**, 492–495.
30 B. P. Binks and S. O. Lumsdon, *Langmuir*, 2000, **16**, 2539–2547.